Hyaluronic Acid-based Inks for Stereolithography (Bio)printing: Benefits of Thiol-ene vs. Acrylate Functionalized Inks

*Therese Steudter[1,2], Tobias Lam[3], Hamidreza Pirmahboub[3], Christian Stoppel[3], Lutz Kloke[3], Samuel Pearson[1], Aránzazu del Campo[1,2]**

[1] INM - Leibniz Institute for New Materials, 66123 Saarbrücken, Germany

[2] Chemistry Department, Saarland University, 66123 Saarbrücken, Germany

[3] Cellbricks GmbH, 13353 Berlin, Germany

*Corresponding author

Email: aranzazu.delcampo@leibniz-inm.de

ABSTRACT

Hydrogel inks used for 3D bioprinting are mainly based on radical polymerization of methacrylate groups. Inks based on the radical thiol-ene polymerization have raised attention in recent years, as they are not susceptible to oxygen inhibition and require lower light doses for polymerization, therefore, they can be more benign to living cells. Here, we modified hyaluronic acid inks with allyl ether or norbornene groups, which can form a crosslinked network in the presence of a dithiol crosslinker. We performed systematic studies to compare precursor stability, photocrosslinking and printability of the thiol-ene inks with methacrylated hyaluronic acid inks. Our results showed

higher storage stability of the thiol-ene hydrogel precursors over 15 months. Photorheology experiments demonstrated faster photocrosslinking and higher temporal control over the network formation in thiol-ene inks. The suitability of thiol-ene inks was demonstrated using digital light processing-based printing with a minimum print time of 2 s per layer and a xy resolution of 100 μm.

KEYWORDS

stereolithography, ink, photocrosslinking, thiol-ene, hydrogel

INTRODUCTION

Digital light processing (DLP) is a (bio)printing technique that allows the fabrication of complex 3D structures.[1–4] The printed scaffolds are fabricated layer-by-layer by projecting a specific pattern onto a liquid photoink which leads to spatially controlled photocrosslinking of the polymeric chains (**Figure 1A**). The printability and the printing resolution achieved with an ink depend on the crosslinking mechanism, the concentration of the functional groups, the viscosity, crosslinking kinetics, and the polymer content.[5] Commonly used polymeric backbones for hydrogel-based (bio)inks are polyethylene glycol (PEG) or natural polymers such as gelatin (GEL) or hyaluronic acid (HA) modified with photocrosslinkable groups.[6–10]

Photocrosslinking most commonly relies on polymerization of (meth)acrylate groups by radical polymerization. Radical polymerization proceeds by a chain growth mechanism and forms heterogeneous networks as the crosslinks consist of new polymer backbones generated by polymerizing through many vinyl groups in an uncontrolled manner (**Figure 1B**).[11] A limitation of radical polymerization of (meth)acrylate groups for DLP printing is the sensitivity of the reaction to the presence of oxygen.[12,13] In bioprinting, the presence of air is inevitable and the inhibition by

oxygen needs to be counteracted by increasing the photoinitiator concentration and by using higher light doses, which compromises cell viability.[12]

Inks based on radical thiol-ene photopolymerization are interesting alternatives to radical (meth)acrylate polymerization. The radical thiol-ene reaction involves the addition of a thiyl radical to a vinyl group to form a thioether (**Figure 1C**). The polymerization proceeds via a step growth mechanism and results in nearly quantitative formation of the corresponding thioether and quantitative consumption of functional groups.[2,12,14] The resulting networks show higher homogeneity than networks polymerized by chain-growth mechanism (**Figure 1D**). The radical thiol-ene reaction is not sensitive to oxygen as the generated peroxy radical readily abstracts a hydrogen atom from a thiol which can then proceed in the thiol-ene polymerization.[12] The kinetics of the addition of the thiyl radical can be tuned by the chemical design of the ene: faster with electron rich or strained vinyl groups like vinyl ether (VE), allyl ether (AE) or norbornene (NB) groups and slower for electron poor vinyl groups or vinyl groups where the intermediate radical is stabilized as in methacrylate (MA).[12,14] Thiol-ene polymerization offers higher conversion than radical polymerization of (meth)acrylate groups and requires lower light doses and fewer radicals [15–17], leading to lower generation of reactive oxygen species and enabling higher cell viability.[18–20]

HA is a non-sulphated glycosaminoglycan present in the extracellular matrix and widely used in biomedical applications. It is biocompatible, non-immunogenic and biodegradable by enzymes like hyaluronidase. The carboxylic acid and alcohol groups on the disaccharide units allow chemical functionalization with photocrosslinkable groups, making them suitable as crosslinked hydrogels for forming stable crosslinked networks with tissue-specific properties.[5,6,8] The viscosity of HA inks can be adjusted by the molecular weight and the polymer concentration. This makes HA inks suitable for 3D printing techniques requiring high viscosity inks like extrusion printing and low viscosity inks like DLP printing. Reported HA inks contain 1.0% w/v to 5.1% wt functionalized

HA (51 to 1700 kDa) with viscosities ranging from 4 to 1000 mPa s (Table S1).[21–28] Light-based 3D printing of methacrylated HA (HA-MA) is often performed in combination with methacrylated GEL (GEL-MA) to introduce cell adhesive sides in the bioprinted scaffold. Such hybrid inks have been used to fabricate 3D tissue models for cartilage[29], liver[30], lungs[31] or vasculature[27] using DLP printing.

HA based thiol-ene inks have been tested in extrusion[25,32], inkjet[21] and DLP[22,26] printing processes. In DLP printing, Dhand et al. used a hybrid ink combining HA-MA with NB-functionalized HA (HA-NB) and dithiol-functionalized admantane-β-cyclodextrin as crosslinker. In combination with lithium-phenyl-2,4,6-trimethylbenzoylphosphinat (LAP) as photoinitiator and tartrazine as photoabsorber, they printed scaffolds with a layer thickness of 100 µm at exposure times of 2.5 s per layer. Thiolated RGD cell adhesive peptide at 2 mM concentration was also included in the bioink and simultaneously linked to NB groups in the network during the printing process.[26] Galarraga et al. used a NB with carboxylic acid substituents to increase the overall hydrophilicity of the NB group which increased the hydrolytic susceptibility of the ester bond between the HA backbone and NB group, rendering the prepared HA-NB gels hydrolytically degradable. Successful DLP printing was achieved with a 5% wt HA-NB ink containing 40% NB functionality and dithioerithrol (DTT) as crosslinker at thiol:ene ratio of 1, 1.7 mM LAP and 1 mM tartrazine. Scaffolds with 100 µm layer thickness and a minimum void space of 500 µm in the xy plane were obtained using 6 s exposure time per layer. Bioinks containing 2 mM thiolated RGD peptide and bovine bone marrow-derived mesenchymal stromal cells allowed printing scaffolds with >80% viability after 3 days.[22]

Although HA based thiol-ene inks have already been tested in DLP printing, existing studies are limited to HA functionalized with NB as ene group and the advantages vs. the commonly used HA-MA ink have not been systematically quantified and compared. Here we synthesized thiol-ene inks

with NB or AE groups and HA-MA derivatives from the same molecular weight HA and similar functionalization degree F_{ene} with the aim to make a comparative study of their storage stability, rheological properties, photocrosslinking kinetics and printability. Our study quantifies the advantages that ene functionalized hydrogel precursors and corresponding thiol-ene based inks can offer in DLP printing.

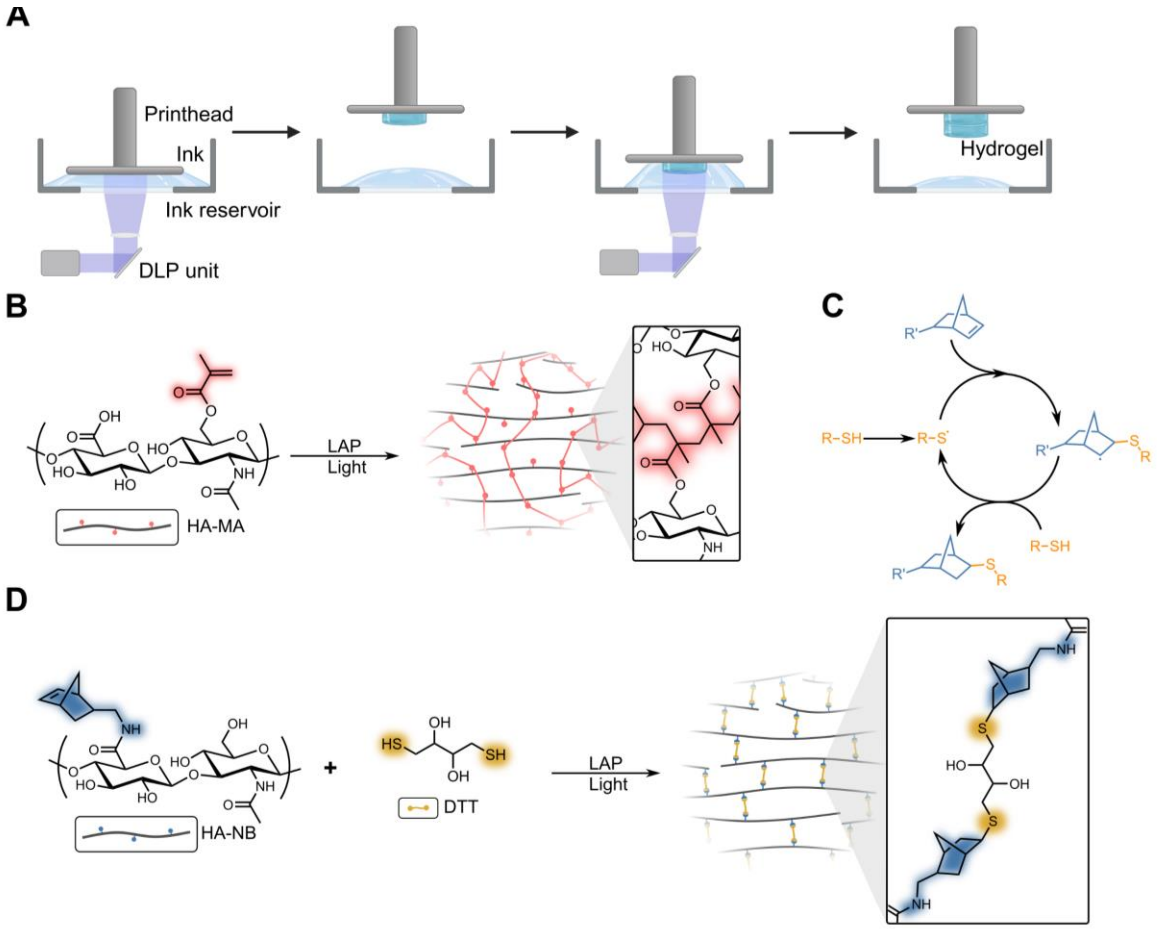

Figure 1. A) Schematic working principle of a DLP printer where the scaffold is printed layer-by-layer. Projection of a photomask through the transparent bottom of the ink reservoir onto the liquid precursor solution leads to spatially controlled photocrosslinking of one layer. Raising the print head and illuminating again photocrosslinks the next layer. Created with BioRender.com **B)** Schematic representation of thiol-ene hydrogel formation: upon irradiation with light and in the

presence of photoinitiator, the dithiol crosslinker DTT reacts with the pendant NB groups on HA to create a crosslinked hydrogel network containing thioethers. **C)** Step-growth mechanism of the radical thiol-ene reaction. **D)** Schematic representation of hydrogel formation with MA groups: radical polymerization of MA groups proceeds via chain growth mechanism leading to multiple crosslinks per group and heterogeneous networks.

MATERIALS AND METHODS

Materials

Hyaluronic acid (purity 97%) with 40-50 kDa molecular weight was purchased from Biosynth s.r.o. (Slovakia). 1-Ethyl-3-(3-dimethylaminopropyl)carbodiimide hydrochloride (EDC, purity ≥99%) was bought from Carbolution Chemicals GmbH (Germany). Allyl glycidyl ether (purity >99.0%) and 5-norbornene-2-methylamine (purity >98.0%) were purchased from TCI Chemicals (Belgium), dithiothreitol (DTT, purity 98%) from abcr GmbH (Germany). D_2O for ^1H NMR spectroscopy was purchased from Deutero (Germany). All other reagents were obtained from Carl Roth GmbH (Germany) and Sigma-Aldrich (Germany). Methacrylated hyaluronic acid was synthesized as described previously.[33]

Synthesis of HA-NB

Norbornene-functionalized hyaluronic acid (HA-NB) was synthesized using EDC/*N*-hydroxysuccinimide (NHS) coupling according to a previously reported protocol by Bian et al.[34] HA (5.00 g, 12.47 mmol disaccharide repeating units) and NHS (2.87 g, 2 eq.) were dissolved at 1% w/v of MilliQ H_2O. After complete dissolution, EDC (9.56 g, 4 eq.) was added as solid and the solution stirred for 2h at room temperature. 5-Norbornene-2-methylamine was added (6.14 g, 4 eq.) to the reaction mixture and stirred at pH = 4.75 for 24 h. During the reaction, pH was adjusted

several times to 4.75 using 1.0 M NaOH and 1.0 M HCl. Subsequently, pH was adjusted to 7.0, NaCl concentration increased to 2 M and the solution precipitated into 1000 mL ice-cold ethanol. After filtration under reduced pressure, the precipitate was washed with ethanol several times and redissolved in 100 mM NaCl at 1% w/v. The solution was transferred in a dialysis bag (MWCO 3.5 kDa, SpectraPor) and dialysed against 100 mM NaCl solution for 24 h and against MilliQ H_2O for 48 h. At last, the solution was lyophilized to obtain HA-NB as solid.

Synthesis of HA-AE

Allyl ether modification of hyaluronic acid was obtained by basic ring opening of allyl glycidyl ether following a previously reported protocol for the synthesis of AE modified dextran.[35] HA (2.5 g, 6.23 mmol disaccharide repeating units) was dissolved at 5% w/v in 0.1 M NaOH and stirred for 30 min. After addition of allyl glycidyl ether (2.1 g, 3 eq.), the solution was stirred at 35 °C for 24 h. The reaction mixture was precipitated in 250 mL ice-cold ethanol and subsequently filtrated and washed as described before. The solid was redissolved in MilliQ H_2O and dialysed against MilliQ H_2O for 48h. Lyophilization yielded HA-AE as white solid.

^{1}H NMR analysis

^{1}H NMR spectra were recorded using a Bruker Avance 300 spectrometer in D_2O at 298 K with a number of scans of 256 and a relaxation delay of 10 s. Chemical shifts are reported in parts per million (δ ppm) with the ^{1}H NMR solvent peak (D_2O: δ = 4.79 ppm) as reference. Analysis of spectra was conducted using Bruker's TopSpin software.

Determination of degree of functionality

To determine degree of alkene functionalization (F_{ene}) of HA-X, ^{1}H NMR spectrum of the polymer dissolved at 15 mg mL^{-1} in D_2O was recorded. Peak area of the acetyl proton signal of hyaluronic acid at 1.97 ppm was compared to the corresponding alkene protons of the attached AE-, NB- or MA groups in the vinyl region (6.30–6.20 ppm). A more detailed description of the functionality calculation can be found in the Supporting Information.

Size exclusion chromatography (SEC)

SEC was performed with a PSS system using a combination of a PSS SUPREMA LUX pre-column and a PSS SUPREMA LUX analytical column equipped with refractive index detector and with 0.07 M Na_2HPO_4 and 20% acetonitrile, pH = 9 as mobile phase.

Precursor stability in storage

To assess storage stability of different HA derivatives, solid polymers were stored at room temperature in the dark. After different time points (t = 0, 4, 8, 12, and 15 months), each derivative was dissolved at 15 mg mL^{-1} in D_2O and ^{1}H NMR spectrum was recorded. In addition, a sample from each timepoint was subjected to SEC analysis.

Calculation of molecular weight per alkene unit

First, the apparent average molar mass of the repeating units in the functionalized hyaluronic acid derivative was calculated by the ratio of the molecular weight (MW) of the native HA repeating unit and the functionalized repeating unit HA-X where X can be either AE, MA or NB depending on the derivative:

$$MW(\text{average}) = MW(\text{HA}) * (1 - F_{\text{ene}}) + MW(\text{HA-X}) * F_{\text{ene}} \quad (1)$$

F_{ene} was the functionality determined for the respective batch. From the average molecular weight per repeating unit, the molecular weight per alkene unit $MW(\text{ene})$ can be calculated as followed:

$$MW(\text{ene}) = \frac{MW(\text{average})}{F_{\text{ene}}} \quad (2)$$

Calculation of thiol concentration for hydrogel precursor solution

In all experiments involving thiol-ene inks, we used equal moles (n) of alkene (ene) and thiol (SH) functional groups:

$$n(\text{ene}) = n(\text{SH}) \quad (3)$$

With a final polymer concentration of c(HA-X) = 4% w/v, the volume V of the solution and the previously calculated molecular weight per alkene unit MW(ene), n(ene) can be re-expressed as

$$n(\text{ene}) = \frac{c(\text{HA}-\text{X}) * V}{MW(\text{ene})} = n(SH) \quad (4)$$

Considering that the used crosslinker is bifunctional and therefore n(SH)=2*n(DTT), the necessary concentration of DTT in the final solution in % w/v can be calculated by

$$c(DTT) = \frac{n(SH) * MW(DTT)}{2 * V} \quad (5)$$

Substitution of eq. 1 for n(SH), c(DTT) can be expressed as

$$c(DTT) = \frac{c(\text{HA}-\text{X}) * MW(DTT)}{2 * MW(\text{ene})} \quad (6)$$

Preparation of hydrogel precursor solution

First, the required amounts of polymer, DTT, LAP and PBS to obtain a 4% w/v HA-X solution were calculated using the functionality F_{ene} and the resulting MW per alkene unit of the specific batch to ensure that the final thiol:ene ratio is 1.00. HA-AE, HA-MA or HA-NB were dissolved in PBS, pH = 7.3 in UV-blocked 50 mL falcons on a shaker at 350 rpm for 60 min. Stock solutions

of LAP (1.0% w/v) and DTT (5.0% w/v) were prepared in PBS and right before the addition the polymer solution to prevent disulfide formation in DTT. To thiol-ene inks, DTT was added as dithiol crosslinker in an equimolar ratio of *n*(SH) and *n*(ene). As last step, the photoinitiator was added to obtain a final concentration of 0.1% w/v.

Crosslinking kinetics and mechanical properties of hydrogels by rheology

Rheological properties and curing kinetics of different hyaluronic-based hydrogels were determined using a rotation rheometer (DHR3, TA Instruments, USA) equipped with a 12 mm parallel plate geometry as upper plate and a transparent lower plate connected to a UV/Vis illumination source (Omnicure, Series 1500) with a 400–500 nm filter to allow in situ curing of hydrogels at room temperature. For each polymer HA-NB, HA-MA and HA-AE, hydrogel precursor solutions were prepared as above. An aliquot was loaded onto the transparent lower plate of the rheometer using a micropipette and the upper parallel plate was lowered to a gap size of 300 µm. The sample was surrounded with silicone oil to prevent evaporation and covered with a metal cover to avoid disturbance during the measurements. Strain sweeps (0.1 to 100% strain at frequency = 2 Hz) and frequency sweeps (0.01 to 100 Hz at strain = 1%) were performed on previously crosslinked hydrogels to determine the linear viscoelastic region. Time sweeps where then carried out in the determined parameters. Storage and loss moduli were recorded over time using 1% applied strain and 2 Hz frequency. For continuous curing measurements, the samples were irradiated with 400–500 nm light (15 mW cm^{-2}) from the 60-s time point onwards using TRIOS software to automatically start the illumination. For sequential curing measurements, the same light source was switched on and off manually. To compare crosslinking kinetics of the different HA derivatives, the gel point t_{gel} where $G' = G''$ was compared. Stiffness of the hydrogels were determined by comparing G' after 20 min of irradiation.

Viscosity measurements

The rheological properties of the uncured precursor solutions were characterized with a modular compact rheometer (MCR, Anton Paar, Austria) was equipped with a 50 mm, 1° cone plate geometry and Peltier stage temperature control system. Temperature was set to 25 °C. First, HA-AE, HA-NB and HA-MA were dissolved at 4% w/v in PBS without photoinitiator and dithiol crosslinker. The solution was placed on the lower plate and the gap lowered to 105 µm. The temperature was held for 1 min and then viscosity was measured in rotational mode at shear rates from 0.1 to 500 s^{-1} at 25 °C.

Determination of degree of thiol-conversion (Ellman's assay)

To quantify the thiol conversion in photocrosslinked thiol-ene hydrogels, we used Ellman's assay to detect free thiols.[36] The protocol was adapted from the manufacturer's instruction. In short, crosslinked hydrogels (20 µL) of HA-AE ($c(SH)_{initial}$ = 39.6 mM) and HA-NB ($c(SH)_{initial}$ = 35.4 mM) were incubated with an excess of a 0.2 mM 5,5'-dithio-bis-(2-nitrobenzoic acid) (DTNB) solution (5 mL) in Ellman's buffer (0.1 M sodium phosphate, 1 mM EDTA, pH = 8.0). Thiol containing standards were prepared by diluting a freshly prepared DTT stock solution (10 mg mL^{-1}, c(SH) = 129.7 mM) with PBS to final concentrations ranging from 0 to 3 mM SH. 20 µL of the standards or hydrogel precursor solutions were incubated along with the hydrogels in 0.2 mM DTNB (1 mL) for 90 min in the dark. 100 µL of supernatant were transferred into a new well plate and the absorbance was measured at 412 nm using a Tecan inifinite 200Pro plate reader. The thiol content in the samples was calculated using the calibration curve prepared by the DTT standards. Finally, the conversion of thiols was determined by comparison of the initial thiol concentration in the hydrogel precursor solution and the thiol content found in the crosslinked hydrogel.

Determination of minimum exposure time per layer in DLP printing

Printing of hydrogel scaffolds was conducted using a DLP based stereolithography printer developed and manufactured by Cellbricks GmbH. The 3D model of the printed scaffold was created using a computer-aided software (CAD) and processed and sliced into different layers by the printer itself. Before each experiment, the printing platform was calibrated to set $z = 0$. Inks for printing experiments was prepared freshly as described before. In addition, the solution was filtered through a 0.45 µm syringe filter and centrifuged to remove any particles or bubbles. Approx. 1 mL ink was loaded into the ink bath consisting of a transparent, hydrophobic foil which allows illumination from the bottom. The constructs were fabricated layer by layer in a stereolithographic process: the first layer was photopolymerized directly on the printing platform and the subsequent layers on top of the previous one by projection of a specific mask with blue light illumination (385 nm, 20 mW/cm^2). After printing one layer, the printing platform was lifted by 1 mm with a speed of 20 mm s^{-1} to then lower in the ink to print the next layer. Each model consisted of three layers (1 mm layer height) resulting in final height of 3 mm with a diameter of 6–9 mm. The printing time per layer t_{layer} was varied to determine the minimum and maximum exposure time per layer. After printing, the scaffold was detached from the printing platform and inspected by eye to determine whether the used exposure time per layer resulted in an undercured, cured or overcured scaffold. The time where the scaffold was no longer undercured but cured i.e. had the desired dimensions of the CAD model, was defined as minimum t_{layer}. The maximum t_{layer} designated the exposure time per layer where the scaffold was cured but higher t_{layer} resulted in overcuring.

Determination of printing resolution

To determine the xy resolution of the different compositions, a CAD model with positive (1000 µm length) and negative (2000 µm length) features with decreasing width (500 to 100 µm length) was designed. Inks were prepared as described before. The CAD model was loaded into the software of the printer, sliced and the printing platform was calibrated. A coverslip with 24 mm diameter was semi-permanently fixed on the printing platform using a photocurable PEG diacrylate ink. The ink was loaded into the vat, the printing platform lowered into the ink and the designated construct printed. The model consisted of one layer (1000 µm layer height) with a length of 13.5 mm and width of 4 mm. After printing, the scaffold was carefully washed with PBS to remove uncured ink, detached from the printing platform, and imaged with a microscope (Leica DMi1, Keyence, Osaka, Japan) equipped with 4x and 10x objectives. Feature sizes were measured using the microscope software.

RESULTS AND DISCUSSION

Bioink formulation

HA solutions exhibit relatively high viscosity due to intra- and interchain hydrophobic interactions and hydrogen bonds.[37] High viscosity can be problematic for SLA printing by restricting flow away from the cured layers and solution refill in the ink reservoir when the printing platform is raised.[38] Successful DLP printing has nonetheless been reported using 88 kDa HA-NB at polymer concentration of 5 wt%,[22] and 1000 kDa HA-MA at a concentration of 1–2% w/v,[27] summarized in Table S1. For our study, we selected HA with a molecular weight of 40–50 kDa and targeted a polymer concentration of 4% w/v for our ink formulation. This molecular weight and concentration are both lower than reported values[22] and viscosity was therefore expected to be low enough for DLP printing.

The reactivity of enes in the radical thiol addition follows the sequence NB > VE > alkene > AE > acrylate > maleimide > MA.[14] This trend largely corresponds to decreasing electron density, with NB particularly reactive due to the release of ring strain and MA particularly unreactive due to intermediate radical stabilization.[14] For our inks we selected the NB and AE groups as -enes with high and intermediate reactivity. In contrast to (meth)acrylate groups, NB and AE groups cannot undergo thiol-Michael addition which ensures that crosslinking proceeds only in the presence of radicals to give high temporal control over the network formation in photoinitiated systems. It also avoids side reactions with other nucleophiles e.g. on the cell surface leading to higher cell viability.[18,23,39–41] In addition, NB and AE groups are not prone to autopolymerisation[42–45] which should increase the polymers' storage stability.

In this work we compared three HA-X derivatives where X stands for the pendant functional group NB, AE or MA. We aimed for HA-X with a F_{ene} of 30–50% to obtain stable hydrogel networks, where F_{ene} is the number of functional groups per HA disaccharide repeating unit. We aimed for thiol-ene inks with high hydrolytic stability so that significant degradation in a cell culture scenario could only occur by the addition of enzymes. We therefore introduced the ene functionalities onto the HA backbone via an amide in HA-NB and an ether bond in HA-AE. These bonds should provide inks which are more stable than ester bonds in HA-MA and cannot be degraded by hydrolysis.

Synthesis of photopolymerizable HA-X

Synthesis and chemical characterization of HA-AE and HA-NB

The syntheses for HA-NB and HA-AE were refined from reported one-step processes in non-toxic solvents.[34,35] To synthesize HA-AE, the primary alcohol group on the C-6 of the *N*-acetyl-d-glucosamine unit in HA was deprotonated in basic medium and reacted with allyl glycidyl ether

through a nucleophilic ring opening reaction (**Scheme 1A**).[35] The functionalized polymer was purified by precipitation and dialysis and lyophilized. The derivatization of the HA was corroborated by ^{1}H NMR spectroscopy. The vinyl protons of AE appeared between 5.15 and 5.36 ppm and confirmed the presence of the allyl group. The F_{ene} was determined by the integral ratio of the vinyl protons relative to the acetyl group of HA (δ = 2.03 ppm) to give F_{ene} = 0.42 ± 0.03. SEC analysis of HA-AE showed no significant differences between the elugrams of HA and HA-AE, indicating that no degradation or crosslinking of the polymeric chains occurred during the synthesis and purification steps (**Figure S2**). By decreasing the equivalents of allyl glycidyl ether in the reaction mixture from 3 to 1.5, HA with a F_{ene} of 0.2 was obtained. HA-AE polymers were soluble in water at tested concentrations up to 5% w/v. For the following studies we used HA-AE with F_{ene} = 0.40–0.47.

HA-NB was prepared by activating the carboxylic acid group of HA with EDC and NHS in H_2O followed by reaction with 5-norbornene-2-methylamine in one step at pH = 4.75. For purification of batches >1 g, an intermediate precipitation step in ethanol was added to remove the excess EDC and reduce dialysis time. For the precipitation in ethanol, the pH and salt concentration in the reaction mixture were adjusted to reported concentrations used for the purification of native HA out of broth (pH = 7.0, 2 M NaCl).[46] This step allowed precipitation of the HA even from solutions at concentrations below 1% w/v, thereby decreasing the dialysis time. The appearance of three peaks in the ^{1}H-NMR spectrum between 5.88 and 6.28 ppm confirmed the successful coupling of NB to the polymer backbone (**Figure S2**). F_{ene} was calculated from the integration of the vinyl protons of NB relative to the acetyl protons of HA (δ = 1.97 ppm). An F_{ene} of 0.41 ± 0.03 was achieved under our reaction conditions. HA-NB with a lower F_{ene} of 0.12 ± 0.03 could be obtained using lower EDC and 5-norbornene-2-methylamine concentrations in the reaction mixture. The

molecular weight distribution of the HA-NB polymer was similar to that of the original HA, indicating that the reaction and purification conditions did not lead to coupling or degradation of the HA chains. The SEC traces did not differ from batches purified by dialysis without precipitation (**Figure S2**). For further experiments, HA batches with F_{ene} = 0.36–0.42 were used. This polymer was soluble in water at all used concentrations.

In contrast to most reported HA-NB syntheses,[21,26,47,48] our EDC/NHS synthesis route is considerably less labour intensive and does not require the use of organic solvents like dimethyl sulfoxide or dimethylformamide. In one popular method, HA is first converted into a tetrabutylammonium salt and then reacted with either 5-norbornene-2-methylamine or 5-norbornene-2-carboxylic acid in dimethyl sulfoxide, requiring up to 14 days of dialysis for purification.[26,47,48] In a different approach, the NB is introduced in two steps by first attaching adipic acid dihydrazide to the carboxylic acid of HA, followed by purification and reaction with *cis*-5-norbonenen-*endo*-2,3-dicarboxylic acid.[21] Our synthesis method only requires one synthesis step and uses water as solvent. A recently published protocol by Plaster et al. uses a similar approach to synthesize HA-NB using an aqueous buffer system and the water-soluble triazine derivative 4-(4,6-dimethoxy-1,3,5-triazin-2-yl) 4-methylmorpholinium chloride as coupling agent.[49]

HA-MA was synthesized as described before.[33] In short, HA was dissolved at 2% w/v in PBS and reacted with methacrylic anhydride for 24 h at 5 °C (**Scheme 1**). For our studies we used HA-MA with F_{ene} = 0.39–0.42.

Scheme 1. Synthesis of HA-X derivatives. (A) HA-NB was synthesized with EDC/NHS coupling and 5-norbornene-2-methylamine, (B) HA-AE was synthesized with allyl glycidyl ether under basic conditions and (C) HA-MA was synthesized using methacrylic anhydride.

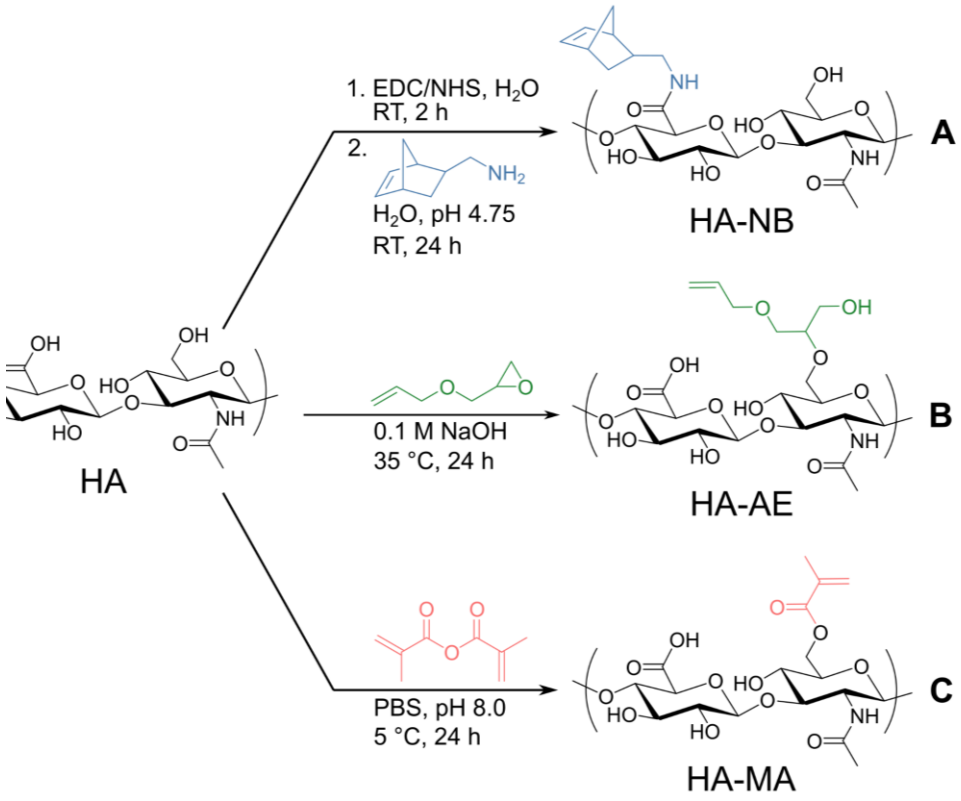

Storage stability of photopolymerizable HA-AE/NB/MA prepolymers

We tested the stability of the synthesized HA derivatives by ^{1}H NMR spectroscopy and SEC analysis. The polymers as solid samples were stored at room temperature in the dark for 15 months. At different time points, solid samples were dissolved at 15 mg mL^{-1} in D_2O and ^{1}H spectra were recorded (**Figure 2**). The NMR spectra of HA-AE and HA-NB showed no changes in the vinyl proton signals in the 15 months, whereas HA-MA showed additional peaks in the spectrum already after 4 months of storage. The stability studies confirm the higher storage stability of hydrogel precursors for thiol-ene inks.

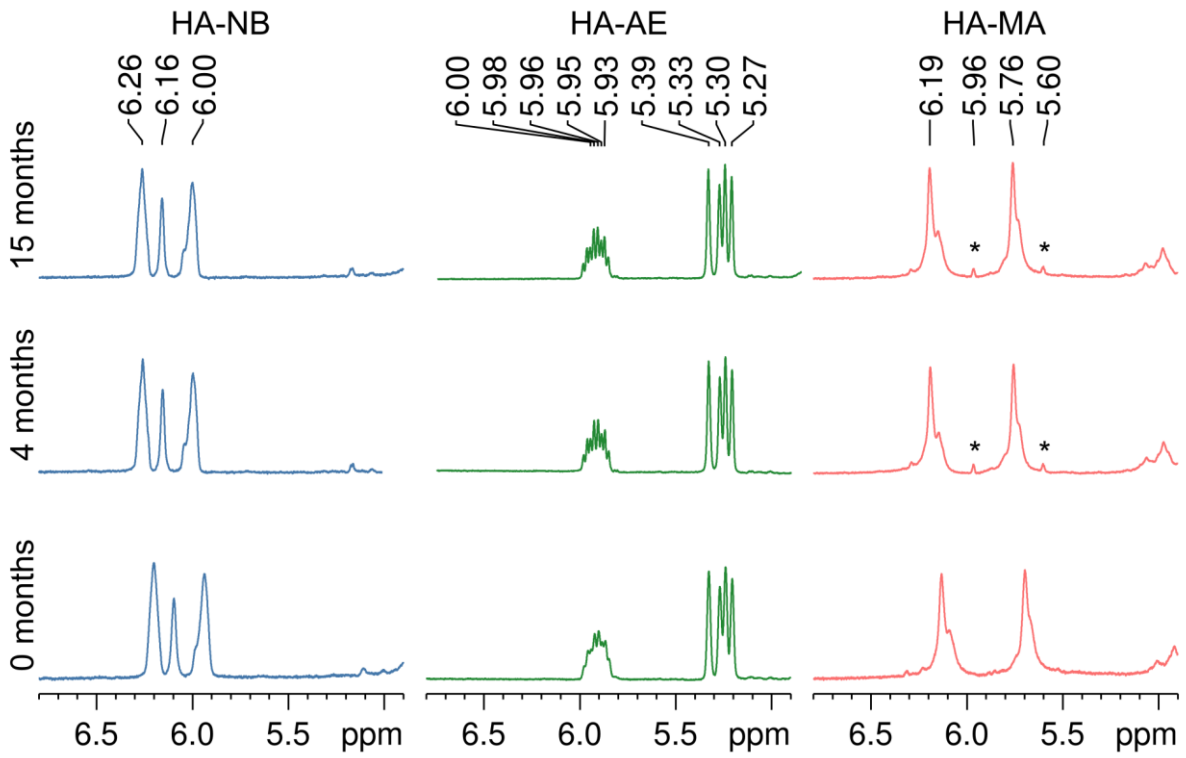

Figure 2. Stability study of HA-X prepolymers over 15 months storage at room temperature in the dark, as measured by ^{1}H NMR. Asterisks indicate the appearance of new signals during storage time.

Viscosity of the inks

DLP printing requires low viscosity inks to ensure the fluid can flow away from the cured material and hollow parts while the printing stage is lifted, and to allow refill of the ink under the raised scaffold for recoating. While literature reports DLP printing of inks with viscosities between 4 mPa s and 2000 mPa s, a viscosity <100 mPa s is more advantageous for good printability.[22,25,27,38,50,51] In our study, HA-X solutions at 4% w/v in PBS showed viscosities well below 100 mPa s (Figure S3) and, therefore, were considered suitable for DLP printing. Within the tested conditions, the inks mostly exhibited a Newtonian behaviour i.e. constant viscosity with varying shear rate which is characteristic of diluted polymer solutions.[23,24,52] While HA-AE possess

an overall lower viscosity than native HA, the viscosity of HA-NB and HA-MA is higher. Introduction of functional groups can change the ionic character and the conformation of the polymeric chains in solution and lead to differences in the viscosity of solutions containing different modified HA derivatives.[53,54]

Study of crosslinking kinetics and mechanical properties by rheology

To investigate the crosslinking kinetics of HA-X hydrogels, we used oscillatory shear rheology and *in situ* illumination at 400–500 nm to initiate photopolymerization. These conditions reflect the typical illumination conditions of DLP printers for bioprinting. **Figure 3A** shows the evolution of the shear moduli with light exposure time. **Table 1** shows the comparative values of the gelation time t_{gel} and the value of the shear modulus at full crosslinking (G'_{20min}) extracted from the curves. t_{gel} is the time needed to reach the gelation point which is defined as the crossover point of storage and loss modulus, $G' = G''$.[55] At the gel point, the polymer solution transitions from a liquid-like (viscous) behaviour to a solid-like (elastic) state corresponding to a three-dimensional network. G'_{20min} reflects the stiffness reached by the hydrogels after crosslinking and 20 min light exposure. The HA-NB ink showed the shortest gelation time ($t_{gel} = 9.0 \pm 0.7$ s) while HA-AE took longer ($t_{gel} = 21.4 \pm 1.2$ s). The rapid reaction of NB is a consequence of the ring strain which is released upon the addition of a thiyl radical.[14] Both HA-NB and HA-AE inks reached a similar value of $G'_{20min} = 8$ kPa, suggesting a similar internal structure of the final network.

The HA-MA showed a different behaviour. The gelation time was longer ($t_{gel} = 42.2 \pm 2.4$ s) and the reached G' value after 20 min of light exposure was approx. 3 times higher than in the thiol-ene crosslinked inks. The longer gelation time can be explained by the different radical polymerisation mechanisms: step-growth polymerization in thiol-ene reaction and chain-growth polymerization in the methacrylate case. Besides the different network growth, oxygen inhibition

can lead to longer gelation times in radical polymerization whereas the thiol-ene reaction is not inhibited by oxygen. The higher stiffness (G'_{20min} = 26 kPa) achieved by HA-MA compared to the thiol-ene hydrogels is attributed to the different network structure resulting from the different polymerization mechanisms. In the radical polymerization of HA-MA each polymerized methacrylate unit links to two neighbours (**Figure 1B**), while in the radical thiol-ene reaction the -ene functions only form a single linkage to the dithiol crosslinker (**Figure 1D**). This leads to a looser network and lower *G*' in the thiol-ene hydrogels.

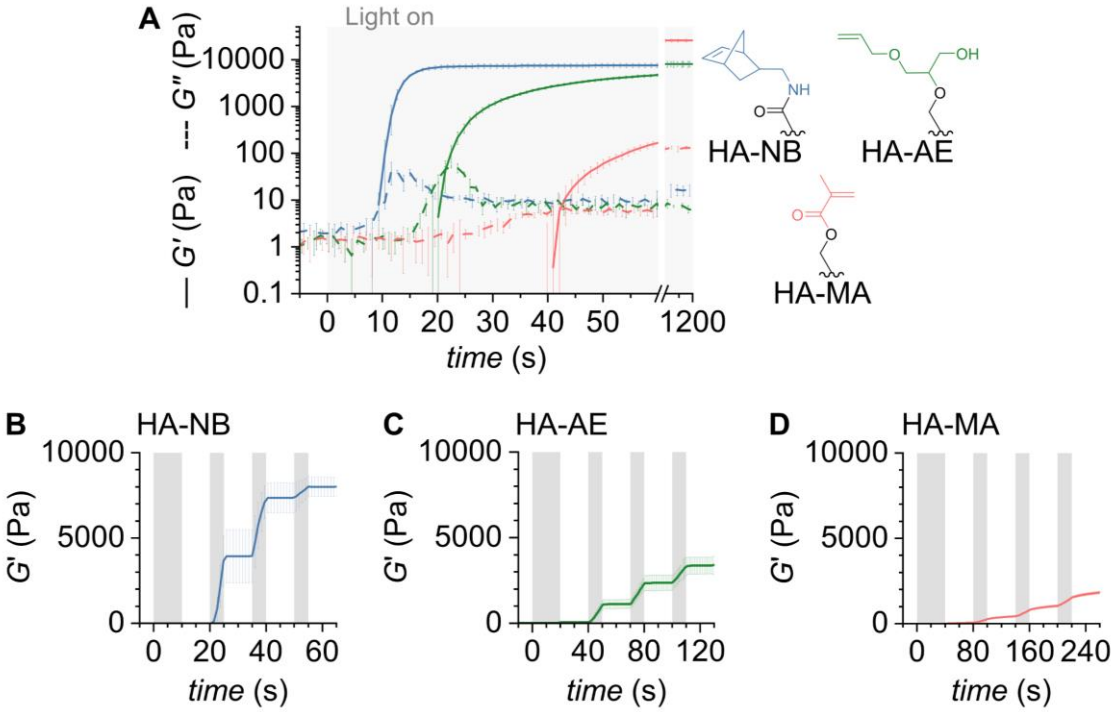

Figure 3. Rheological characterization of HA-X ink photocuring. **A)** Evolution of storage modulus *G*' (continuous line) and loss modulus *G*" (dashed line) of HA-X precursor solutions during photocrosslinking (400–500 nm, 15 mW cm^{-2}). Exposure started at t = 0 s. **B–D)** Evolution of storage modulus of HA-X hydrogel precursor solutions upon sequential irradiation at 400–500 nm, 15 mW cm^{-2}. Shaded boxes indicate the periods where the light was switched on. Polymers were dissolved at 4% w/v in PBS. Solutions contained 0.1% w/v LAP as photoinitiator. The thiol-ene solutions HA-AE and HA-NB contained DTT as crosslinker at 1:1 thiol:ene ratio. N = 3.

Table 1. The composition, gel point t_{gel} and storage modulus $G'_{20\ min}$ of different HA-X precursor solutions determined by oscillatory shear rheology and *in situ* illumination. All samples contained 0.1% w/v LAP as photoinitiator.

HA-X	F_{ene}	$c_{HA\text{-}X}$ (% w/v)	c_{DTT} (% w/v)	t_{gel} (s)	$G'_{20\ min}$ (kPa)
HA-NB	0.36	4.0	0.27	9.0 ± 0.7	8.1 ± 0.9
HA-AE	0.46	4.0	0.35	21.4 ± 1.2	8.0 ± 1.2
HA-MA	0.39	4.0	-	42.2 ± 2.4	25.5 ± 2.0

In a photoinitiated radical polymerization, tuning the light intensity and illumination profile allow control over the crosslinking progress. This was tested in two different experiments. HA-NB inks were exposed to 365-nm light of increasing irradiance between 1 and 6 mW cm^{-2}. At 6 mW cm^{-2} gelation occurred in less than 1 s. Decreasing the irradiance to 1 mW cm^{-2} increased the gelation time to approx. 5 s (**Figure S4**). We also monitored the crosslinking during step-wise exposure with 400–500-nm light at 15 mW cm^{-2} (**Figure 3B,C**). Thiol-ene crosslinked hydrogels showed an increase of *G*' during the illumination periods and a constant *G*' during the dark periods, indicating that the crosslinking starts and stops with the light exposure. This offers precise temporal control over the network formation. In contrast, the storage modulus in the HA-MA system also increased after the light was switched off. This indicates that the macroradicals in the forming network do not undergo a fast termination and continue to propagate in the dark phase provided there are still available vinyl groups.

Calculation of the conversion of the thiol-ene polymerization reaction by quantification of the free thiol end groups

The degree of crosslinking in a thiol-ene crosslinked hydrogel can be quantified by reacting the free thiol groups with the Ellman's reagent, DTNB.[21,26,36] The reaction leads to a disulfide and a free TNB anion that absorbs at 412 nm. We found a thiol conversion of 77 and 78% in HA-AE and HA-NB hydrogels prepared with stochiometric concentrations of thiol and ene functions after full exposure. The incompleteness of the crosslinking reaction is attributed to the limited mobility of the dithiol crosslinkers once attached to a HA chain by one end, which reduces their probability to meet remaining alkene groups at more distant positions in the network. Such free thiols can be exploited for post-polymerization functionalization of the hydrogels.[36]

DLP-based SLA printing

We tested the printability of the HA-X inks using a DLP printer. The following formulation was used in the printing experiments: 4.0% w/v HA-X, 0.1% w/v LAP, and for the thiol-ene inks, DTT at a thiol:ene ratio of 1.

Determination of printing speed

We first printed layers of 1-mm thickness to complete a 3-layered disc with a diameter of 6–9 mm. The exposure time per layer was increased between 1 and 50 s and the resulting discs were imaged to compare the dimensions and the contours of the disc. Undercured prints showed smaller-than-targeted dimensions while overcured prints showed larger-than-targeted dimensions and oblique walls. **Figure 4** shows representative images of HA-X scaffolds printed with different exposure times.

Using HA-NB ink, a minimum exposure time per layer (t_{layer}) of 2 s gave a printed scaffold with the targeted dimensions, while HA-MA required t_{layer} of 10 s. Surprisingly, the minimum t_{layer} for HA-AE was also 10 s which did not reflect its faster curing vs HA-MA found in photorheology experiments. The reason for this difference is not known at this point. HA-NB allowed 5-fold faster

printing compared to HA-MA, which is comparable to the fold-difference obtained for t_{gel} of the two inks in photo-rheology experiments. The significantly faster printing of HA-NB is particularly interesting in bioprinting, where shorter exposure times minimize cellular photodamage and the time cells are exposed to an environment outside of ideal growth and incubation conditions. This is especially important for bioprinting with sensitive cells and for fabricating large and complex scaffolds.

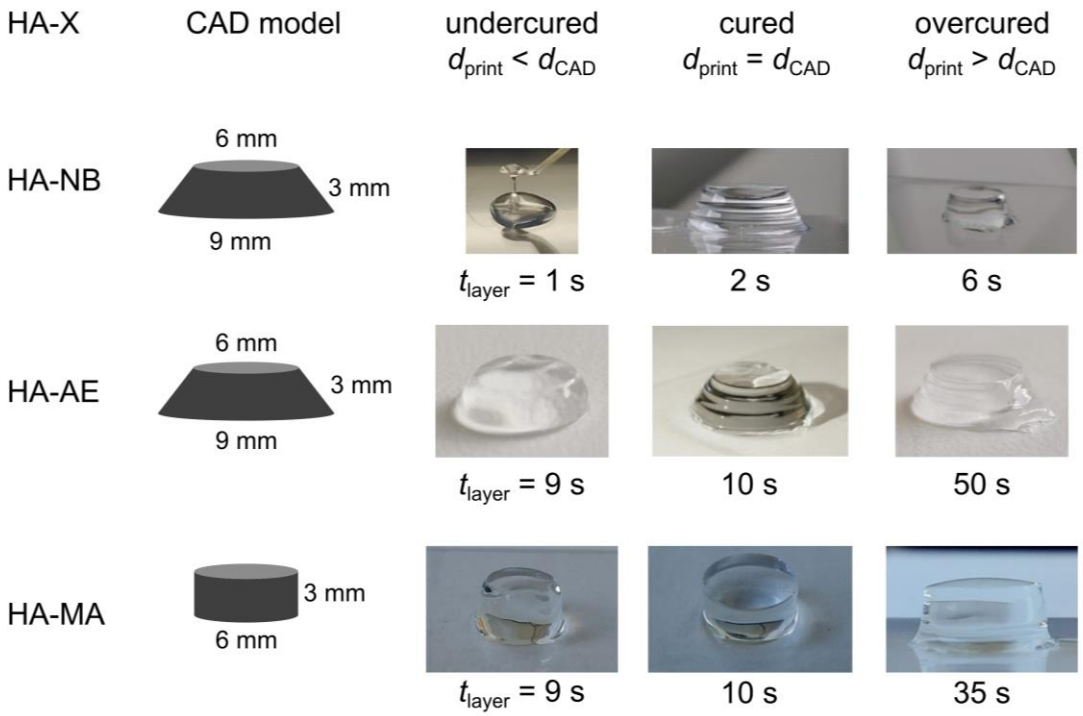

Figure 4. Determination of minimum and maximum exposure time t_{layer} for HA-X hydrogels. Comparison of the printed structure to the CAD model allowed qualitive assessment of undercured, cured and overcured prints.

Determination of xy resolution

Printing resolution defines minimum feature size that can be printed. In DLP-based 3D printing, resolution depends on the diffusion rate of the reactive species inside the ink, the kinetic of the

crosslinking reaction and on the magnification of the light source (i.e. pixel size).[5] To achieve high resolution in the printed structure, the crosslinking reaction ideally occurs fast to limit diffusion of the reactive species outside of the illuminated zone.[57]

To test the spatial resolution of printed scaffolds obtained from thiol-ene based inks, we printed single 1000-µm thick layers containing rectangular positive and negative features which we refer to as protrusions and channels. Protrusions were 1 mm long and channels were 2 mm long, and their widths decreased from 500 to 100 µm (**Figure 5A**). To avoid damage of the scaffold during handling, the structures were printed directly on coverslips attached to the printing platform. HA-NB was printed with t_{layer} = 2.7 s. The microscopy image of the printed structure shows well defined features down to 100 µm width with good dimensional agreement with the theoretical size in the CAD model (**Figure 5B,C**). HA-NB therefore allows printing of structures with high resolution and high shape fidelity. To our knowledge, this is the smallest printed feature size demonstrated with hyaluronic acid-based inks in DLP printing. Previous studies reported a maximum xy resolution in the range of 250–400 µm using hyaluronic acid based inks and DLP printing (**Table S1**).[22,26,27]

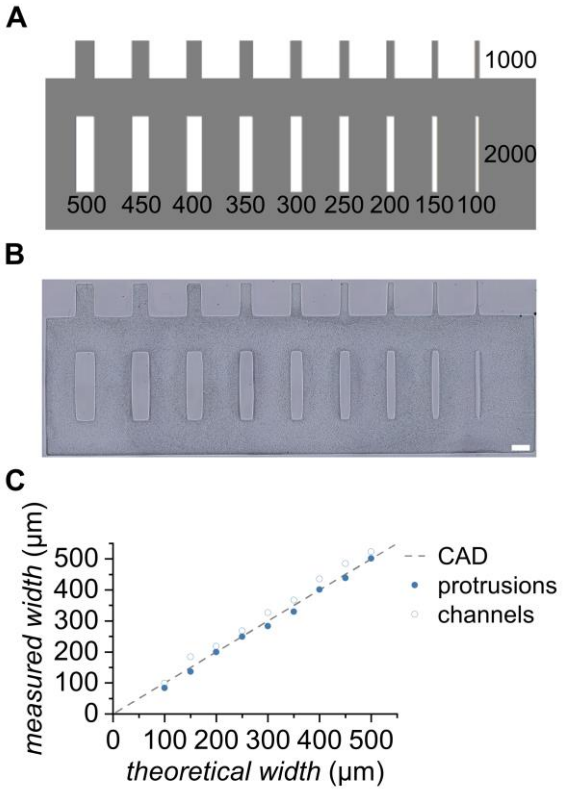

Figure 5. Printing resolution experiments. **A)** CAD model used to print scaffolds for determination of xy resolution. The widths of the positive and negative features are stated in µm. **B)** Microscopy images of printed HA-NB scaffold with 1000 µm layer height. Scale bar represents 500 µm. **C)** Measured width for protrusions (closed symbols) and channels (open symbols) for the HA-NB scaffolds printed with 1000 µm layer height compared to the theoretical width of the CAD model (dashed line).

CONCLUSIONS

In this work, HA-based thiol-ene inks carrying AE or NB functions were prepared, and their photocrosslinking behaviour was compared with that of the commonly used methacrylated ink HA-MA. The syntheses of HA-AE and HA-NB were optimized to obtain the polymers in one step under aqueous conditions and to decrease the time and solvent required for dialysis. In photorheology and DLP printing studies, HA-NB crosslinked over 4 times faster than HA-MA.

Both thiol-ene inks showed higher temporal control over the network formation, with stiffness only increasing during illumination while the stiffness of the HA-MA network continued to rise in the dark state between illumination periods. Because of the different network structures, the stiffness of the thiol-ene hydrogels was lower than in the methacrylated ones after extended curing. Scaffolds were printed with feature sizes down to 100 μm. This detailed insight into the photocuring behaviour and printing performance of HA-based thiol-ene inks will support efforts to design bioprinted scaffolds with optimized print times and mechanical properties.

ASSOCIATED CONTENT

Supporting Information

Representative ^{1}H NMR spectra of HA-NB, HA-AE and HA-MA; representative SEC elugrams of HA-NB and HA-AE; viscosity measurements of HA-X polymer solutions; photorheology of HA-NB precursor solution at 365 nm with different light intensities; selected reports using HA-X inks for 3D printing.

AUTHOR INFORMATION

Corresponding Author

*Aránzazu del Campo − INM − Leibniz Institute for New Materials, 66123 Saarbrücken, Germany; Saarland University, Chemistry Department, 66123 Saarbrücken, Germany; orcid.org/0000-0001-5725-2135; Email: aranzazu.delcampo@leibniz-inm.de

Author Contributions

The manuscript was written through contributions of all authors. All authors have given approval to the final version of the manuscript.

Funding Sources

The research reported in this publication was supported by the Bundesministerium für Bildung und Forschung (BMBF, Germany).

Notes

The authors declare no competing financial interest.

ACKNOWLEDGMENTS

We thank Ha Rimbach-Nguyen (INM) for SEC measurements. Parts of the table of contents graphic were created using BioRender.com.

REFERENCES

(1) Derakhshanfar, S.; Mbeleck, R.; Xu, K.; Zhang, X.; Zhong, W.; Xing, M. 3D Bioprinting for Biomedical Devices and Tissue Engineering: A Review of Recent Trends and Advances. *Bioact. Mater.* **2018**, *3*, 144–156.

(2) Lim, K. S.; Galarraga, J. H.; Cui, X.; Lindberg, G. C. J.; Burdick, J. A.; Woodfield, T. B. F. Fundamentals and Applications of Photo-Cross-Linking in Bioprinting. *Chem. Rev. (Washington, DC, U. S.)* **2020**, *120*, 10662–10694.

(3) Mandrycky, C.; Wang, Z.; Kim, K.; Kim, D. H. 3D Bioprinting for Engineering Complex Tissues. *Biotechnol. Adv.* **2016**, *34*, 422–434.

(4) Skoog, S. A.; Goering, P. L.; Narayan, R. J. Stereolithography in Tissue Engineering. *J. Mater. Sci.: Mater. Med.* **2014**, *25*, 845–856.

(5) Sekar, M. P.; Suresh, S.; Zennifer, A.; Sethuraman, S.; Sundaramurthi, D. Hyaluronic Acid as Bioink and Hydrogel Scaffolds for Tissue Engineering Applications. *ACS Biomater. Sci. Eng.* **2023**, *9*, 3134–3159.

(6) Burdick, J. A.; Prestwich, G. D. Hyaluronic Acid Hydrogels for Biomedical Applications. *Adv. Mater.* **2011**, *23*, H41–H56.

(7) Choi, J. R.; Yong, K. W.; Choi, J. Y.; Cowie, A. C. Recent Advances in Photo-Crosslinkable Hydrogels for Biomedical Applications. *BioTechniques* **2019**, *66*, 40–53.

(8) Iaconisi, G. N.; Lunetti, P.; Gallo, N.; Cappello, A. R.; Fiermonte, G.; Dolce, V.; Capobianco, L. Hyaluronic Acid: A Powerful Biomolecule with Wide-Ranging Applications—A Comprehensive Review. *Int. J. Mol. Sci.* **2023**, *24*.

(9) Puertas-Bartolomé, M.; Mora-Boza, A.; García-Fernández, L. Emerging Biofabrication Techniques: A Review on Natural Polymers for Biomedical Applications. *Polymers* **2021**, *13*, 1209.

(10) Teixeira, M. C.; Lameirinhas, N. S.; Carvalho, J. P. F.; Silvestre, A. J. D.; Vilela, C.; Freire, C. S. R. A Guide to Polysaccharide-Based Hydrogel Bioinks for 3D Bioprinting Applications. *Int. J. Mol. Sci.* **2022**, *23*, 6564.

(11) Lin, C. C.; Ki, C. S.; Shih, H. Thiol-Norbornene Photo-Click Hydrogels for Tissue Engineering Applications. *J. Appl. Polym. Sci.* **2015**, *132*.

(12) Cramer, N. B.; Bowman, C. N. CHAPTER 1. Thiol-ene and Thiol-yne Chemistry in Ideal Network Synthesis. In *Thiol-X Chemistries in Polymer and Materials Science*; Polymer Chemistry Series; 2013; pp 1–27.

(13) Simič, R.; Mandal, J.; Zhang, K.; D. Spencer, N. Oxygen Inhibition of Free-Radical Polymerization Is the Dominant Mechanism behind the "Mold Effect" on Hydrogels. *Soft Matter* **2021**, *17*, 6394–6403.

(14) Lowe, A. B. Thiol-Ene "Click" Reactions and Recent Applications in Polymer and Materials Synthesis. *Polym. Chem.* **2010**, *1*, 17–36.

(15) Anseth, K. S.; Burdick, J. A. New Directions in Photopolymerizable Biomaterials. *MRS Bull.* **2002**, *27*, 130–136.

(16) Shih, H.; Lin, C.-C. Visible-Light-Mediated Thiol-Ene Hydrogelation Using Eosin-Y as the Only Photoinitiator. *Macromol. Rapid Commun.* **2013**, *34*, 269–273.

(17) Van Hoorick, J.; Gruber, P.; Markovic, M.; Rollot, M.; Graulus, G.-J.; Vagenende, M.; Tromayer, M.; Van Erps, J.; Thienpont, H.; Martins, J. C.; Baudis, S.; Ovsianikov, A.; Dubruel, P.; Van Vlierberghe, S. Highly Reactive Thiol-Norbornene Photo-Click Hydrogels: Toward Improved Processability. *Macromol. Rapid Commun.* **2018**, *39*, 1800181.

(18) Gockler, T.; Haase, S.; Kempter, X.; Pfister, R.; Maciel, B. R.; Grimm, A.; Molitor, T.; Willenbacher, N.; Schepers, U. Tuning Superfast Curing Thiol-Norbornene-Functionalized Gelatin Hydrogels for 3D Bioprinting. *Adv. Healthcare Mater.* **2021**, *10*, 2100206.

(19) Mũnoz, Z.; Shih, H.; Lin, C.-C. Gelatin Hydrogels Formed by Orthogonal Thiol–Norbornene Photochemistry for Cell Encapsulation. *Biomater. Sci.* **2014**, *2*, 1063–1072.

(20) Zhao, C.; Wu, Z.; Chu, H.; Wang, T.; Qiu, S.; Zhou, J.; Zhu, Q.; Liu, X.; Quan, D.; Bai, Y. Thiol-Rich Multifunctional Macromolecular Crosslinker for Gelatin-Norbornene-Based Bioprinting. *Biomacromolecules* **2021**, *22*, 2729–2739.

(21) Acosta-Velez, G. F.; Linsley, C. S.; Craig, M. C.; Wu, B. M. Photocurable Bioink for the Inkjet 3D Pharming of Hydrophilic Drugs. *Bioengineering* **2017**, *4*, 11/1.

(22) Galarraga, J. H.; Dhand, A. P.; Enzmann, B. P. I.; Burdick, J. A. Synthesis, Characterization, and Digital Light Processing of a Hydrolytically Degradable Hyaluronic Acid Hydrogel. *Biomacromolecules* **2023**, *24*, 413–425.

(23) Hauptstein, J.; Forster, L.; Nadernezhad, A.; Horder, H.; Stahlhut, P.; Groll, J.; Blunk, T.; Tessmar, J. Bioink Platform Utilizing Dual-Stage Crosslinking of Hyaluronic Acid Tailored for Chondrogenic Differentiation of Mesenchymal Stromal Cells. *Macromol. Biosci.* **2022**, *22*, 2100331.

(24) Ouyang, L.; Highley, C. B.; Rodell, C. B.; Sun, W.; Burdick, J. A. 3D Printing of Shear-Thinning Hyaluronic Acid Hydrogels with Secondary Cross-Linking. *ACS Biomater. Sci. Eng.* **2016**, *2*, 1743–1751.

(25) Galarraga, J. H.; Kwon, M. Y.; Burdick, J. A. 3D Bioprinting via an in Situ Crosslinking Technique towards Engineering Cartilage Tissue. *Sci. Rep.* **2019**, *9*, 19987.

(26) Dhand, A. P.; Davidson, M. D.; Galarraga, J. H.; Qazi, T. H.; Locke, R. C.; Mauck, R. L.; Burdick, J. A. Simultaneous One-Pot Interpenetrating Network Formation to Expand 3D Processing Capabilities. *Adv. Mater.* **2022**, *34*, 2202261.

(27) Thomas, A.; Orellano, I.; Lam, T.; Noichl, B.; Geiger, M.-A.; Amler, A.-K.; Kreuder, A.-E.; Palmer, C.; Duda, G.; Lauster, R.; Kloke, L. Vascular Bioprinting with Enzymatically

Degradable Bioinks via Multi-Material Projection-Based Stereolithography. *Acta Biomater.* **2020**, *117*, 121–132.

(28) Poldervaart, M. T.; Goversen, B.; de Ruijter, M.; Abbadessa, A.; Melchels, F. P. W.; Öner, F. C.; Dhert, W. J. A.; Vermonden, T.; Alblas, J. 3D Bioprinting of Methacrylated Hyaluronic Acid (MeHA) Hydrogel with Intrinsic Osteogenicity. *PLoS One* **2017**, *12*, e0177628.

(29) Lam, T.; Dehne, T.; Krüger, J. P.; Hondke, S.; Endres, M.; Thomas, A.; Lauster, R.; Sittinger, M.; Kloke, L. Photopolymerizable Gelatin and Hyaluronic Acid for Stereolithographic 3D Bioprinting of Tissue-Engineered Cartilage. *J. Biomed. Mater. Res., Part B* **2019**, *107*, 2649–2657.

(30) Grix, T.; Ruppelt, A.; Thomas, A.; Amler, A. K.; Noichl, B. P.; Lauster, R.; Kloke, L. Bioprinting Perfusion-Enabled Liver Equivalents for Advanced Organ-on-a-Chip Applications. *Genes* **2018**, *9*.

(31) Hossain Rakin, R.; Kumar, H.; Rajeev, A.; Natale, G.; Menard, F.; Li, I. T. S.; Kim, K. Tunable Metacrylated Hyaluronic Acid-Based Hybrid Bioinks for Stereolithography 3D Bioprinting. *Biofabrication* **2021**, *13*.

(32) Song, K. H.; Highley, C. B.; Rouff, A.; Burdick, J. A. Complex 3D-Printed Microchannels within Cell-Degradable Hydrogels. *Adv. Funct. Mater.* **2018**, *28*, 1801331.

(33) Shopperly, L. K.; Spinnen, J.; Krüger, J.-P.; Endres, M.; Sittinger, M.; Lam, T.; Kloke, L.; Dehne, T. Blends of Gelatin and Hyaluronic Acid Stratified by Stereolithographic Bioprinting Approximate Cartilaginous Matrix Gradients. *J. Biomed. Mater. Res., Part B* **2022**, *110*, 2310–2322.

(34) Bian, S.; He, M.; Sui, J.; Cai, H.; Sun, Y.; Liang, J.; Fan, Y.; Zhang, X. The Self-Crosslinking Smart Hyaluronic Acid Hydrogels as Injectable Three-Dimensional Scaffolds for Cells Culture. *Colloids Surf., B* **2016**, *140*, 392–402.

(35) Li, M.; Tang, Z.; Wang, C.; Zhang, Y.; Cui, H.; Chen, X. Efficient Side-Chain Modification of Dextran via Base-Catalyzed Epoxide Ring-Opening and Thiol-Ene Click Chemistry in Aqueous Media. *Chin. J. Polym. Sci.* **2014**, *32*, 969–974.

(36) Sawicki, L. A.; Kloxin, A. M. Light-Mediated Formation and Patterning of Hydrogels for Cell Culture Applications. *J. Visualized Exp.* **2016**, No. 115, e54462.

(37) Fallacara, A.; Baldini, E.; Manfredini, S.; Vertuani, S. Hyaluronic Acid in the Third Millennium. *Polymers* **2018**, *10*, 701.

(38) Choi, J. W.; Kim, G.-J.; Hong, S.; An, J. H.; Kim, B.-J.; Ha, C. W. Sequential Process Optimization for a Digital Light Processing System to Minimize Trial and Error. *Sci. Rep.* **2022**, *12*, 13553.

(39) Heffernan, J. M.; Overstreet, D. J.; Le, L. D.; Vernon, B. L.; Sirianni, R. W. Bioengineered Scaffolds for 3D Analysis of Glioblastoma Proliferation and Invasion. *Ann. Biomed. Eng.* **2015**, *43*, 1965–1977.

(40) Nair, D. P.; Podgórski, M.; Chatani, S.; Gong, T.; Xi, W.; Fenoli, C. R.; Bowman, C. N. The Thiol-Michael Addition Click Reaction: A Powerful and Widely Used Tool in Materials Chemistry. *Chem. Mater.* **2014**, *26*, 724–744.

(41) Wan, T.; Fan, P.; Zhang, M.; Shi, K.; Chen, X.; Yang, H.; Liu, X.; Xu, W.; Zhou, Y. Multiple Crosslinking Hyaluronic Acid Hydrogels with Improved Strength and 3D Printability. *ACS Appl. Bio Mater.* **2022**, *5*, 334–343.

(42) Bermeshev, M. V.; Chapala, P. P. Addition Polymerization of Functionalized Norbornenes as a Powerful Tool for Assembling Molecular Moieties of New Polymers with Versatile Properties. *Prog. Polym. Sci.* **2018**, *84*, 1–46.

(43) Jensen, E. S.; Gatenholm, P.; Nanguneri, S. R.; Mathias, L. J. Effect of Chemical Structure of Allyl Ethers on Polymerization and Properties of Multifunctional Acrylate Systems. *J. Appl. Polym. Sci.* **1991**, *42*, 2681–2689.

(44) Jian, Z.; Mecking, S. Insertion Homo- and Copolymerization of Diallyl Ether. *Angew. Chem., Int. Ed.* **2015**, *54*, 15845–15849.

(45) Rajaraman, S. K.; Crivello, J. V. Novel Tandem Isomerization/ Cationic Polymerization of Allyl Ethers. *Des. Monomers Polym.* **1998**, *1*, 77–88.

(46) Cavalcanti, A. D. D.; Melo, B. A. G.; Oliveira, R. C.; Santana, M. H. A. Recovery and Purity of High Molar Mass Bio-Hyaluronic Acid Via Precipitation Strategies Modulated by pH and Sodium Chloride. *Appl. Biochem. Biotechnol.* **2019**, *188*, 527–539.

(47) Gramlich, W. M.; Kim, I. L.; Burdick, J. A. Synthesis and Orthogonal Photopatterning of Hyaluronic Acid Hydrogels with Thiol-Norbornene Chemistry. *Biomaterials* **2013**, *34*, 9803–9811.

(48) Wang, C.; Hao, H.; Wang, J.; Xue, Y.; Huang, J.; Ren, K.; Ji, J. High-Throughput Hyaluronic Acid Hydrogel Arrays for Cell Selective Adhesion Screening. *J. Mater. Chem. B* **2021**, *9*, 4024–4030.

(49) Plaster, E. M.; Eiken, M. K.; Loebel, C. DMTMM-Mediated Synthesis of Norbornene-Modified Hyaluronic Acid Polymers to Probe Cell-Hydrogel Interactions. *Carbohydr. Polym. Technol. Appl.* **2023**, *6*, 100360.

(50) Caprioli, M.; Roppolo, I.; Chiappone, A.; Larush, L.; Pirri, C. F.; Magdassi, S. 3D-Printed Self-Healing Hydrogels via Digital Light Processing. *Nat. Commun.* **2021**, *12*, 2462.

(51) Shahzadi, L.; Maya, F.; Breadmore, M. C.; Thickett, S. C. Functional Materials for DLP-SLA 3D Printing Using Thiol–Acrylate Chemistry: Resin Design and Postprint Applications. *ACS Appl. Polym. Mater.* **2022**, *4*, 3896–3907.

(52) Rebenda, D.; Vrbka, M.; Čípek, P.; Toropitsyn, E.; Nečas, D.; Pravda, M.; Hartl, M. On the Dependence of Rheology of Hyaluronic Acid Solutions and Frictional Behavior of Articular Cartilage. *Materials* **2020**, *13*, 2659.

(53) Borke, T.; Najberg, M.; Ilina, P.; Bhattacharya, M.; Urtti, A.; Tenhu, H.; Hietala, S. Hyaluronic Acid Graft Copolymers with Cleavable Arms as Potential Intravitreal Drug Delivery Vehicles. *Macromol. Biosci.* **2018**, *18*, 1700200.

(54) Guo, L.; Chai, Y.; Zhou, F.; Wang, P. Preparation and Properties of Hyaluronic Acid Hydrogel Modified by L-Cysteine Hydrochloride. *IOP Conf. Ser.: Earth Environ. Sci.* **2021**, *651*, 042022.

(55) Tung, C.-Y. M.; Dynes, P. J. Relationship between Viscoelastic Properties and Gelation in Thermosetting Systems. *J. Appl. Polym. Sci.* **1982**, *27*, 569–574.

(56) Winter, H. H.; Mours, M. Rheology of Polymers Near Liquid-Solid Transitions. In *Neutron Spin Echo Spectroscopy Viscoelasticity Rheology*; Advances in Polymer Science; Springer: Berlin, Heidelberg, 1997; pp 165–234.

(57) Xue, D.; Zhang, J.; Wang, Y.; Mei, D. Digital Light Processing-Based 3D Printing of Cell-Seeding Hydrogel Scaffolds with Regionally Varied Stiffness. *ACS Biomater. Sci. Eng.* **2019**, *5*, 4825–4833.

TABLE OF CONTENTS GRAPHIC

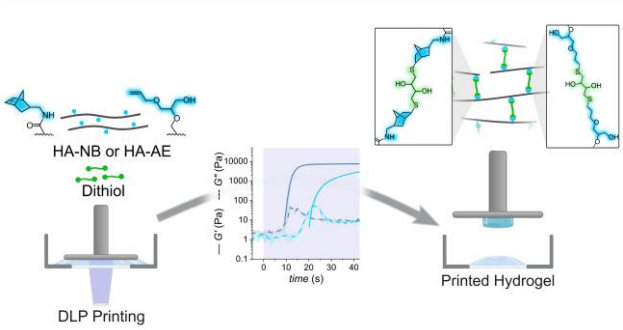

Supporting Information

Hyaluronic Acid-based Inks for Stereolithography (Bio)printing: Benefits of Thiol-ene vs. Acrylate Functionalized Inks

*Therese Steudter[1,2], Tobias Lam[3], Hamidreza Pirmahboub[3], Christian Stoppel[3], Lutz Kloke[3], Samuel Pearson[1], Aránzazu del Campo[1,2]**

[1] INM - Leibniz Institute for New Materials, Saarbrücken, Germany

[2] Chemistry Department, Saarland University, 66123 Saarbrücken, Germany

[3] Cellbricks GmbH, 13353 Berlin, Germany

*Corresponding author

Email: aranzazu.delcampo@leibniz-inm.de

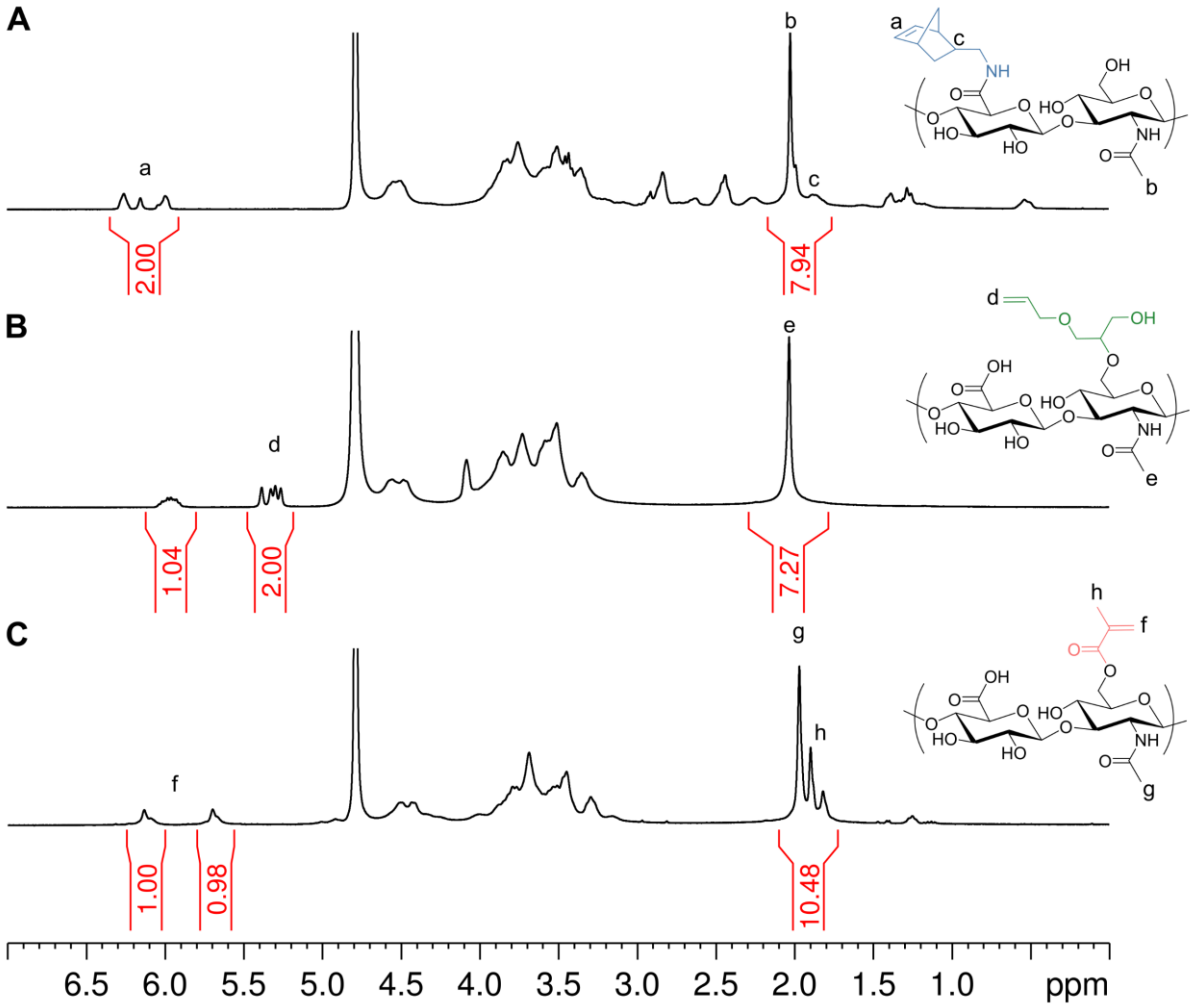

Figure S1. ^{1}H NMR spectra of A) HA-NB, B) HA-AE, and C) HA-MA in D_2O. For A), the vinyl proton 'a' from the norbornene group (6.26–6.00 ppm) were set as reference to I_a = 2.00 meaning that the number of norbornene groups was n = 2.00 / 2 = 1.00. The number of hyaluronic acid protons was determined by integrating the signal of the acetyl protons 'b' and the quaternary proton of norbornene 'c' (2.03–1.87 ppm) by subtracting the integral of the latter one found in the starting material 5-norbornene-2-methylamine where I_c = 0.84. This value is smaller than 1 because the used 5-norbornene-2-methylamine contains both, endo- and exo isomers. This results in a number of hyaluronic acid disaccharide units of $m = (I_{b+c} - I_c) / 3 = (7.94 - 0.84) / 3 = 2.37$. Comparing the ratio of norbornene groups versus the number of HA repeating units gives a functionality of $F_{ene} = n / m = 1.00 / 2.37 = 0.42$. For B), the integral of vinyl protons signal 'd' from the allyl ether group (5.38–5.26 ppm) was set as reference to I_d = 2.00 which corresponds to $n = I_d / 2 = 2.00 / 2 = 1.00$ allyl ether groups. The integral protons 'e' from the acetyl group in *N*-acetyl-D-glucosamine (2.03 ppm) were used to calculate the number of hyaluronic acid repeating

units *m*, i.e. $m = I_d / 3 = 7.27 / 3 = 2.42$. The F_{ene} was then calculated by calculating the ratio between allyl ether groups *n* and HA repeating units *m*, i.e. $F_{ene} = n / m = 1.00 / 2.42 = 0.41$. For C), the one of the two vinyl protons 'f' from the methacrylate group (6.12 ppm) was used as reference with $I_e = 1.00$ corresponding to $n = I_e / 1 = 1.00 / 1 = 1.00$ methacrylate groups grafted onto to the polymer backbone. The integral of the proton signals f–g (1.97–1.82 ppm) is used to calculate the number of the HA repeating units *m* by subtracting the methyl protons e of the methacrylate group, i.e. $m = I_f / 3 = (I_{f+g} - 3) / 3 = (10.48 - 3) / 3 = 2.49$. The ratio of methacrylate groups *n* and HA repeating units determined the functionality to be $F_{ene} = n / m = 1.00 / 2.49 = 0.40$.

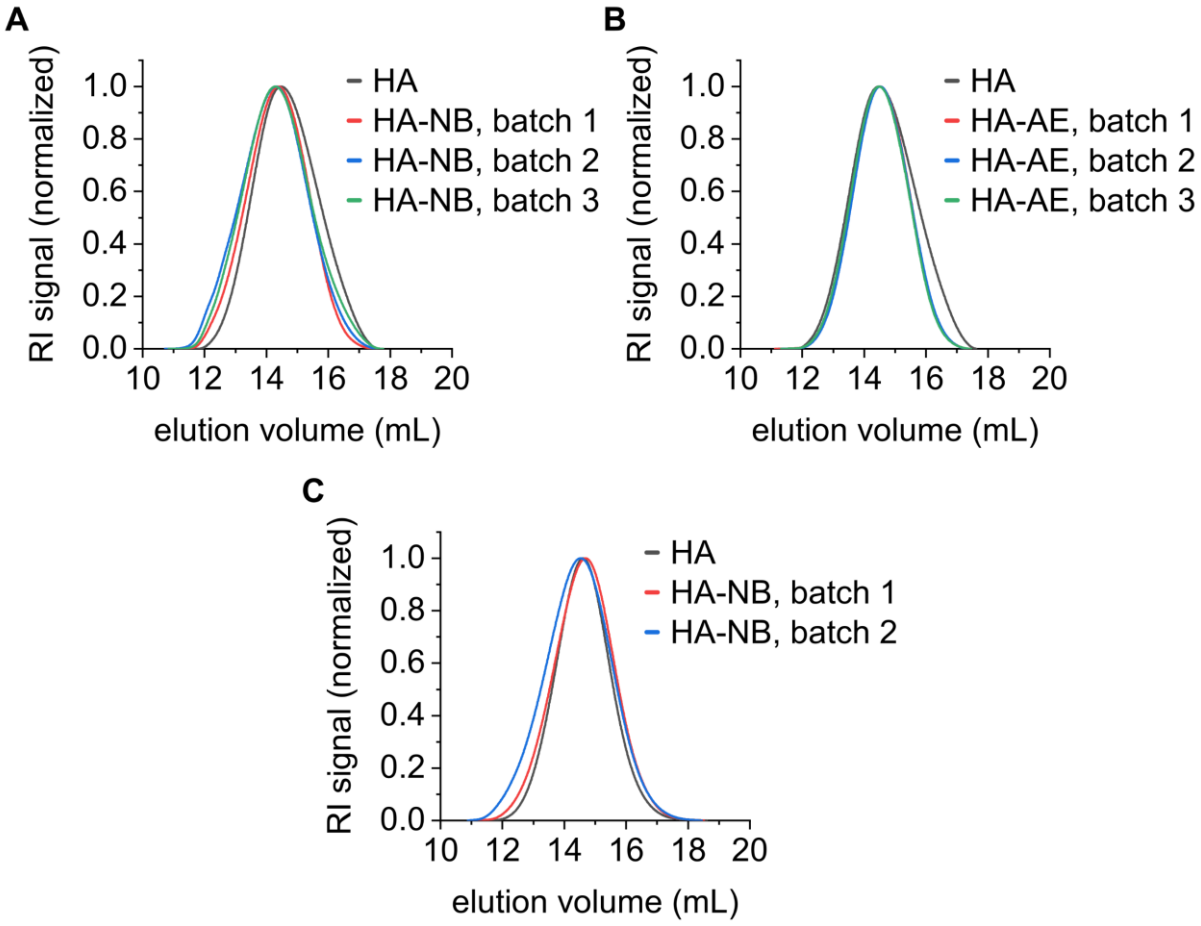

Figure S2. Representative SEC elugrams of different HA-NB and HA-AE batches purified by precipitation (A–B) and dialysis (C).

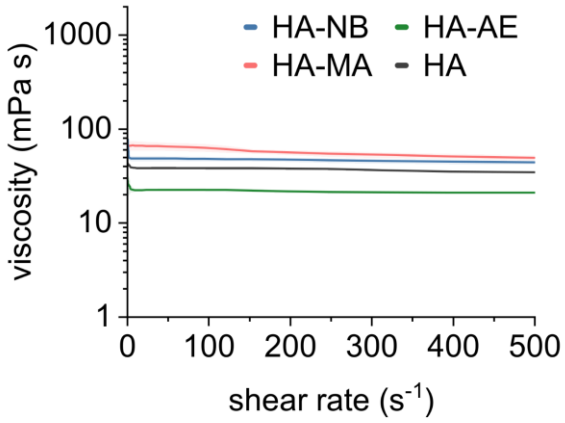

Figure S3. Viscosity measurement of HA-X derivatives as function of the shear rate.

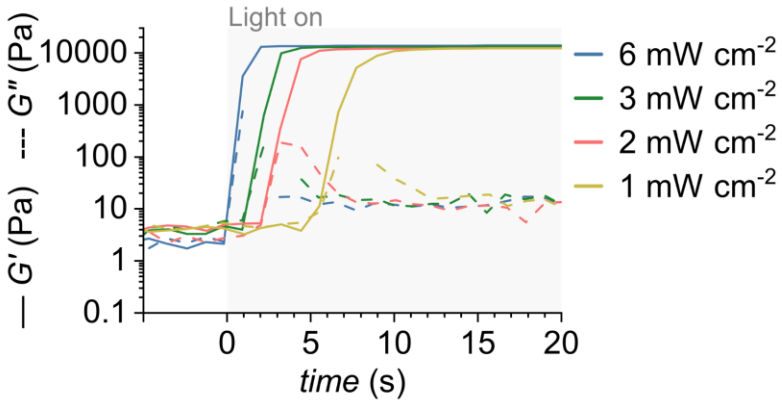

Figure S4. Evolution of storage modulus *G*' (continuous line) and loss modulus *G*" (dashed line) of HA-NB precursor solutions during photocrosslinking with light (365 nm) with light intensities between 1–6 mW cm^{-2} (N = 1). Exposure started at t = 0 s.

Table S1. Physicochemical properties of HA inks used for printing in selected reports.

Reactive group	F_{ene} (%)	MW_{HA} (kDa)	[HA-X]	Crosslinker	Printing technique	Viscosity (mPa s)	Storage Modulus G' (kPa)	Young's Modulus E (kPa)	xy Resolution (µm)	Ref.
NB	50	60	3% w/w	PEG2SH	inkjet	8	0.8	-	-	[1]
NB	40	74	2% w/w	DTT	extrusion	-	~ 6	-	-	[2]
MA	100	88	0.6% w/w	dithiol-functionalized admantane-*β*-cyclodextrin	DLP	~60 [a)]	~14 (IPN) ~11 (HA-NB only)	-	~250	[3]
NB	40		4.5% w/w							
NB	40	88	5% w/w	DTT	DLP	~200 [a)]	~0.01	-	~400	[4]
MA	14	1000	1-2% w/v	-	DLP	4-13 [a)]	-	1.3-4.5	~360	[5]
MA	22	90	5%	-	extrusion	<1000	~11	-	-	[6]
MA	5-7	1700	3% w/v	-	extrusion	-	2.6	-	-	[7]
SH	45	51	2.5% w/v	PEGDA PEG-di-allyl	extrusion	~10	-	~5	-	[8]
NB	36-42	40-50	4% w/v	DTT	DLP	~20-60 [a)]	8-27	-	~100	This study
AE	40-47									
MA	39-42			-						

a) at 100 s^{-1} shear rate

REFERENCES

(1) Acosta-Velez, G. F.; Linsley, C. S.; Craig, M. C.; Wu, B. M. Photocurable Bioink for the Inkjet 3D Pharming of Hydrophilic Drugs. *Bioengineering* **2017**, *4*, 11/1.

(2) Galarraga, J. H.; Kwon, M. Y.; Burdick, J. A. 3D Bioprinting via an in Situ Crosslinking Technique towards Engineering Cartilage Tissue. *Sci. Rep.* **2019**, *9*, 19987.

(3) Dhand, A. P.; Davidson, M. D.; Galarraga, J. H.; Qazi, T. H.; Locke, R. C.; Mauck, R. L.; Burdick, J. A. Simultaneous One-Pot Interpenetrating Network Formation to Expand 3D Processing Capabilities. *Adv. Mater.* **2022**, *34*, 2202261.

(4) Galarraga, J. H.; Dhand, A. P.; Enzmann, B. P. I.; Burdick, J. A. Synthesis, Characterization, and Digital Light Processing of a Hydrolytically Degradable Hyaluronic Acid Hydrogel. *Biomacromolecules* **2023**, *24*, 413–425.

(5) Thomas, A.; Orellano, I.; Lam, T.; Noichl, B.; Geiger, M.-A.; Amler, A.-K.; Kreuder, A.-E.; Palmer, C.; Duda, G.; Lauster, R.; Kloke, L. Vascular Bioprinting with Enzymatically Degradable Bioinks via Multi-Material Projection-Based Stereolithography. *Acta Biomater.* **2020**, *117*, 121–132.

(6) Ouyang, L.; Highley, C. B.; Rodell, C. B.; Sun, W.; Burdick, J. A. 3D Printing of Shear-Thinning Hyaluronic Acid Hydrogels with Secondary Cross-Linking. *ACS Biomater. Sci. Eng.* **2016**, *2*, 1743–1751.

(7) Poldervaart, M. T.; Goversen, B.; de Ruijter, M.; Abbadessa, A.; Melchels, F. P. W.; Öner, F. C.; Dhert, W. J. A.; Vermonden, T.; Alblas, J. 3D Bioprinting of Methacrylated Hyaluronic Acid (MeHA) Hydrogel with Intrinsic Osteogenicity. *PLoS One* **2017**, *12*, e0177628.

(8) Hauptstein, J.; Forster, L.; Nadernezhad, A.; Horder, H.; Stahlhut, P.; Groll, J.; Blunk, T.; Tessmar, J. Bioink Platform Utilizing Dual-Stage Crosslinking of Hyaluronic Acid Tailored for Chondrogenic Differentiation of Mesenchymal Stromal Cells. *Macromol. Biosci.* **2022**, *22*, 2100331.